

A Novel Control Strategy for On-Grid Photovoltaic Systems Based on Adaptive PI Control

A.H. Azad, H. Shateri

Department of Electrical and Computer Engineering
Arak University of Technology
Arak, Iran

a.azad@arakut.ac.ir, shateri@arakut.ac.ir

Abstract– This paper presents a novel control strategy for grid-connected photovoltaic system based on adaptive PI. The proposed control strategy has following steps: implementation of beta algorithm for maximum power point tracking (MPPT) in photovoltaic system; dc link voltage stabilization; and grid current control utilizing model reference adaptive control (MRAC-PI) method. In the proposed control method, the coefficients of PI are continuously estimated based on MIT rule in order to decrease error between reference values and controlling variables. Simulation results of the proposed controller confirm the robust performance in uncertainty of irradiance. Comparing with optimized classic PI controllers, utilizing PSO algorithm, proposed controller has a better performance in the both transient and steady state conditions.

Index Terms– Grid-connected photovoltaic system, Model Reference Adaptive Control - PI (MRAC-PI), MPPT, Beta method.

I. INTRODUCTION

In recent years, solar energy has a high growth rate compared to other renewable energy resources, due to its advantages, such as clean energy source, low production cost, and the feasibility to be installed as an on-grid or off-grid (distributed generation in faraway areas) [1]. As mentioned in [2], the total installed solar energy capacity in the world provides 2.1% of the world's electrical energy consumption. The average cost of production per watt of solar energy in the world (including tax) in 2018 is \$3.14. Fig. 1 shows the total installed solar energy in the world [1-2].

Due to numerous advantages of PV systems and their high popularity, several efforts are oriented to implementation and controlling of this systems. Therefore, there are various technics for PV systems operation. In the following, on-grid PV systems configurations are classified based on their inverter topology and control system.

A. On-Grid PV Energy Conversion Systems Configurations

On-grid photovoltaic energy conversion systems configurations are divided into four categories based on converter's topology. Each structure can be classified into some sub-classes based on connection status between PV and dc link, utilizing or not utilizing transformers, and the type of applied converters. The detailed comparison between various sub-class and different converters type is given in [3-4]. TABLE I provides a summarized classification of various structures.

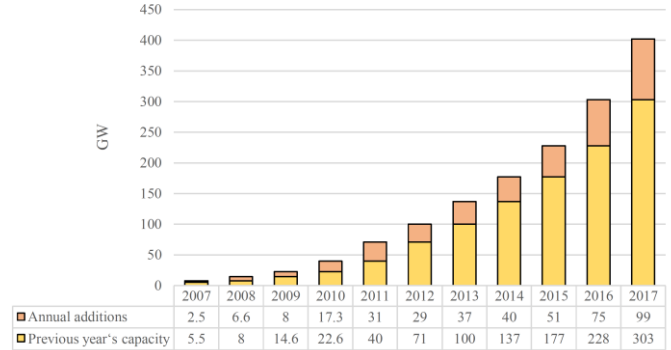


Fig. 1. Solar PV Global Capacity and Annual Additions, 2007-2017 [1-2]

In this paper, a structure from class “string” from type “d” is utilized. This structure applies a two-level Voltage Source Inverter (VSL-2L) and a boost converter.

B. On-Grid PV System Control Strategies

Control strategies presented for controlling on-grid PV system can be summarized as shown in Fig. 2. In the mentioned classified methods, PI controller [5], proportional resonance (PR) controller [6], sliding mode controller (SMC) [7-9], feedback linearization (FL) controller [10], adaptive controller [11-12] are common in PV system applications.

In [5-6] PI and PR controllers are applied for grid current control respectively, and both have used PI controller for controlling dc link voltage of on-grid PV system. In spite of wide application of PI and PR controllers, duo to simplicity of designing, controller performance in nonlinear and in any form of uncertainty could face to many problems.

In [9] SMC is applied for controlling d and q components of grid current and a PI controller is utilized for a three-phase on-grid converter. Providing suitable responses, simplicity of

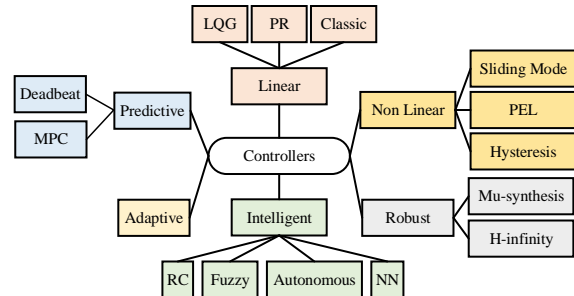


Fig. 2. On-grid PV systems classification due to their control strategies [5-15]

TABLE I. SUMMARY OF GRID-CONNECTED PV SYSTEM CONFIGURATIONS [3-4]

Scale	Small		Medium	Large
Topologies	ac-module	String	Multi-String	Central
Characteristics				
Convert Efficiency	Up to 96.5%	Up to 97.8%	Up to 98%	Up to 98.6%
Features	Easy installation Highest MPPT efficiency Higher losses Higher cost per watt	Reduced dc wiring Good MPPT efficiency Transformerless 1-String and 1-Inverter	Flexible/Modular High MPPT efficiency	Simple structures Poor MPPT efficiency Non-flexible
Configuration				

designing, robustness against uncertainties are the advantages of this controller. However, chattering in controller entrance limits the application of this controller.

In [10], a robust FL controller is proposed for controlling grid current and dc link voltage in on-grid PV system. By omitting nonlinear components from on-grid system by this controller, a simple linear PI controller can be utilized for system. Complexity in designing of this controller and dependence of this method on PV system parameters, limits the application of this controller.

In [13], an adaptive controller is utilized for dc link voltage regulation; and in [14] an adaptive controller is used for network power factor controlling in a three-phase on-grid converter, which operates as a reactive power compensator (SVC). In spite of robust and flexible performance of adaptive control method, some problems such as complexity in design of high order systems, non-identified theoretical solution routine and accurate selection of controlling constants, limits application of this control method.

Although the above mentioned control systems improve PI controller performance, but most of them suffer from the problem of complexity in design and control constants tuning [15].

II. MATHEMATICAL MODELLING OF ON-GRID PV SYSTEM

On-grid PV system is shown in Fig. 3. Power-Voltage characteristic of PV arrays are presented in (1) for a PV array with N_p parallel modules and N_s series modules:

$$P_{PV} = N_p V_{PV} I_{ph} - N_p V_{PV} I_s \left[\exp\left(\frac{V_{PV} + R_s I_{PV}}{N_s V_t}\right) - 1 \right] - \left(\frac{V_{PV}^2 + R_s I_{PV} V_{PV}}{R_p} \right) \quad (1)$$

where V_{PV} , I_{PV} , I_{ph} , R_s , R_p , V_t are output voltage and current of PV, photocurrent: the current resulted from irradiance on each

cell, series resistor, parallel resistor, and thermal voltage, respectively. Dynamic equations of on-grid three-phase inverter in abc frame is presented in (2) and in dq frame in (3).

$$\begin{cases} L \frac{dI_a}{dt} = -RI_a - V_a + U_a \\ L \frac{dI_b}{dt} = -RI_b - V_b + U_b \\ L \frac{dI_c}{dt} = -RI_c - V_c + U_c \\ C_b \frac{dV_{dc}}{dt} = \frac{U_a I_a + U_b I_b + U_c I_c}{V_{dc}} \end{cases} \quad (2)$$

Defining $U_{dc} = \frac{C_b}{3V_d} V_{dc}^2$ and due to zero value of q component of grid voltage, dynamic equation of dc link voltage can be rewritten as:

$$\begin{cases} \frac{dI_d}{dt} = \frac{-R}{L} I_d + \omega I_q + \frac{U_d}{L} - \frac{V_d}{L} \\ \frac{dI_q}{dt} = \frac{-R}{L} I_q - \omega I_d + \frac{U_q}{L} - \frac{V_q}{L} \\ \frac{dV_{dc}}{dt} = \frac{3}{2} \frac{V_d I_d + V_q I_q}{C_b V_{dc}} \end{cases} \quad (3)$$

$$\frac{dU_{dc}}{dt} = -\frac{2}{C_b} U_{dc} + I_d \quad (4)$$

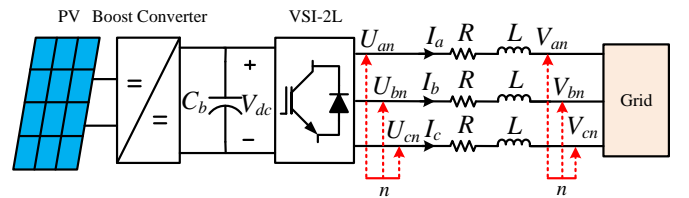


Fig. 3. Block diagram of on-grid PV system

III. PROPOSED CONTROLLING SYSTEM

The proposed control system consists of three sections: MPPT control unit, dc link voltage stabilizer unit, and grid current control unit. Beta algorithm is utilized to achieve maximum power extraction from PV system. Furthermore, model reference of adaptive control-PI (MRAC-PI) is used for dc link voltage stabilizing and control of grid current. In the proposed control system, PI controller coefficients are estimated online applying MIT rules, in such a way that the steady state error of three control variables of V_{dc} , I_d , and I_q become zero. The advantages of the proposed control system are acceptable response in transient and steady state conditions in presence of variation in irradiance. It should be mentioned that the proposed controller is suitable for large variation in irradiance and it is applicable on large scale PV systems.

A. Maximum Power Point Tracking (MPPT) Algorithm

The proposed Beta algorithm in [16] is utilized to achieve maximum power point tracking in PV arrays. Flowchart of this algorithm is shown in Fig. 4.

B. Grid-Connected Inverter Control

MRAC-PI controller based on MIT rules is utilized for controlling grid current and dc link voltage. Diagram of this controller is shown in Fig. 5. In Fig. 5, y , y_m , e , y_{ref} , and u are system model output, reference model output, error of the models, the reference value, and input of transfer function, respectively. In order to design the proposed controller, dynamic equations of grid current in dq frame, which were mentioned in (3), are rewritten as:

$$\begin{cases} \frac{dI_d}{dt} = \frac{-R}{L} I_d + u_d \\ \frac{dI_q}{dt} = \frac{-R}{L} I_q + u_q \end{cases} \quad (5)$$

where, U_d and U_q are outputs of MRAC-PI controller in d and q axis direction, respectively, and they are defined as:

$$\begin{aligned} u_d &= +\omega I_q + \frac{U_d}{L} - \frac{V_d}{L} \\ u_q &= -\omega I_d + \frac{U_q}{L} - \frac{V_q}{L} \end{aligned} \quad (6)$$

MRAC-PI controller outputs can be described as:

$$\begin{aligned} u_d &= K_{P,d}(I_{d,ref} - I_d) + K_{I,d} \int (I_{d,ref} - I_d) dt \\ u_q &= K_{P,q}(I_{q,ref} - I_q) + K_{I,q} \int (I_{q,ref} - I_q) dt \end{aligned} \quad (7)$$

According to (5) and (7), transform function of grid current in d axis and q axis are as following:

$$\frac{I_d}{I_{d,ref}} = \frac{K_{P,d}s + K_{I,d}}{s^2 + \left(\frac{R}{L} + K_{P,d}\right)s + K_{I,d}} \quad (8)$$

$$\frac{I_q}{I_{q,ref}} = \frac{K_{P,q}s + K_{I,q}}{s^2 + \left(\frac{R}{L} + K_{P,q}\right)s + K_{I,q}} \quad (9)$$

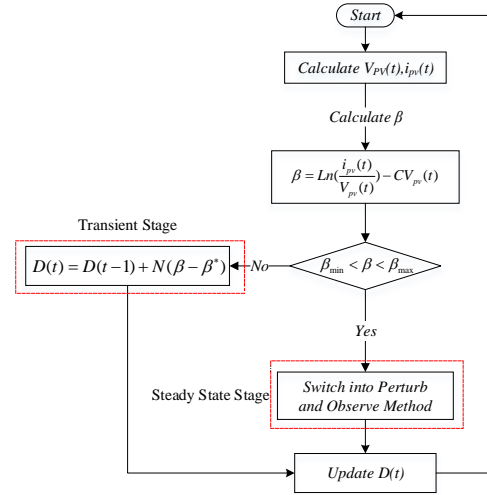


Fig. 4. Flowchart of the Beta method [16]

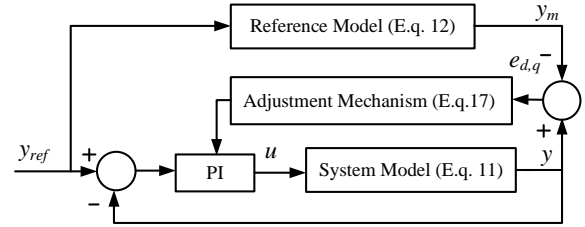


Fig. 5. Proposed controller (MRAC-PI) diagram based on MIT rules

I_d is the output of dc link PI controller. Output of this controller can be described as:

$$I_d = K_{P,vdc}(V_{dc,ref} - V_{dc}) + K_{I,vdc} \int (V_{dc,ref} - V_{dc}) dt \quad (10)$$

Transform function of dc link voltage can be determined according to (4) and (10):

$$\frac{V_{dc}}{V_{dc,ref}} = \frac{K_{P,vdc}s + K_{I,vdc}}{s^2 + \left(\frac{2}{C_b} + K_{P,vdc}\right)s + K_{I,vdc}} \quad (11)$$

According to same order of closed loop transfer function of I_d , I_q , and V_{dc} , their closed loop transfer function can be written as (12), and reference model can be described as (13). Parameters of reference model for each control parameter are evaluated with target of improving time response.

$$\frac{y}{u} = \frac{b_p(K_P s + K_I)}{a_0 s^2 + (a_1 + b_p K_P)s + b_p K_I} \quad (12)$$

$$\frac{y_m}{u_m} = \frac{b_{m_1}s + b_{m_2}}{a_{m_0}s^2 + a_{m_1}s + a_{m_2}} \quad (13)$$

MIT rule is based on minimizing the defined cost function for error between the real model and reference model. This is represented in (14):

$$J(\theta) = \frac{1}{2} e^2 \quad (14)$$

where θ represent the controlling parameters. In order to minimize J , θ should be changed in opposite direction of J guardian.

$$\frac{d\theta}{dt} = -\gamma \cdot e \cdot \frac{de}{d\theta} \quad (15)$$

According to (15), updating rules of system PI coefficients mentioned in (13), can be calculated as:

$$\begin{aligned} \frac{dK_p}{dt} &= -\gamma_{KP} \cdot \frac{dJ}{dK_p} = -\gamma_{KP} \cdot \frac{dJ}{de} \cdot \frac{de}{dy} \cdot \frac{dy}{dK_p} = -\gamma_{KP} \cdot e \cdot \frac{dy}{dK_p} \\ \frac{dK_I}{dt} &= -\gamma_{KI} \cdot \frac{dJ}{dK_I} = -\gamma_{KI} \cdot \frac{dJ}{de} \cdot \frac{de}{dy} \cdot \frac{dy}{dK_I} = -\gamma_{KI} \cdot e \cdot \frac{dy}{dK_I} \end{aligned} \quad (16)$$

In (16), $\frac{dy}{dK_p}$ and $\frac{dy}{dK_I}$ are calculated as:

$$\begin{aligned} \frac{dy}{dK_p} &= \left[\frac{b_p s}{s^2 + (a_1 + b_p K_p) s + b_p K_I} \right] [y_{ref} - y] \\ \frac{dy}{dK_I} &= \left[\frac{b_p}{s^2 + (a_1 + b_p K_p) s + b_p K_I} \right] [y_{ref} - y] \end{aligned} \quad (17)$$

Since coefficients a_1 and b_p in (17), coefficients of the main transform function, are not known they should be estimated according to real transform function. By replacing (17) in (16), updating equations of PI can be evaluated as:

$$\begin{aligned} \frac{dK_p}{dt} &= -\gamma_{KP} \cdot e \cdot \left[\frac{b_p s}{s^2 + (a_1 + b_p K_p) s + b_p K_I} \right] [y_{ref} - y] \\ \frac{dK_I}{dt} &= -\gamma_{KI} \cdot b_p \cdot e \cdot \left[\frac{y_{ref} - y}{s^2 + (a_1 + b_p K_p) s + b_p K_I} \right] \end{aligned} \quad (18)$$

IV. SIMULATION AND RESULTS

Diagram of the proposed control algorithm is shown in Fig. 6. On-grid PV system (Fig. 3) performance with the proposed control system is simulated and results are compared with PI controller, which its coefficients are optimized by PSO algorithm (the same as [5]). Specifications of arrays of PV system are mentioned in TABLE II. Specifications of grid-connected PV system are given in TABLE III.

TABLE II. NOMINAL PARAMETERS USED IN SIMULATION

Parameters	Values	Parameters	Values
Ambient temp.	25°C	V_{MPP}	283 V
Irradiance	1000 W/m ²	I_{MPP}	19.8 A
V_{oc}	353 V	I_{sc}	21.16 A

TABLE III. GENERAL PARAMETERS OF GRID-CONNECTED PV SYSTEM

Parameters	Values	Parameters	Values
V_{grid}	220 V	L_{grid}	23 mH
C_{dc}	3.3 mF	$L_{Boost-Conv}$	5 mH
V_{dc}	500 V	R_{filter}	0.05 Ω

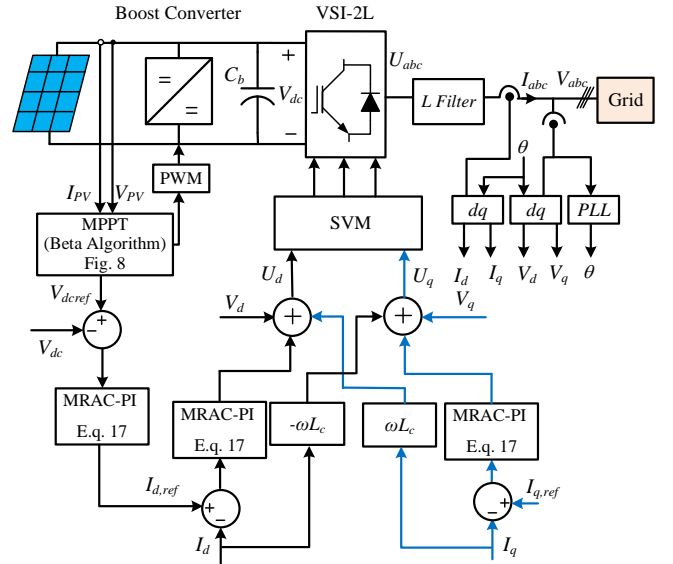


Fig. 6. Block diagram of proposed control (MRAC-PI)

Power-Voltage characteristic of PV arrays used in on-grid photovoltaic system is shown in Fig. 7. DC link voltage controlled by PI controller and the proposed controller (MARC-PI) are illustrated in Fig. 8.

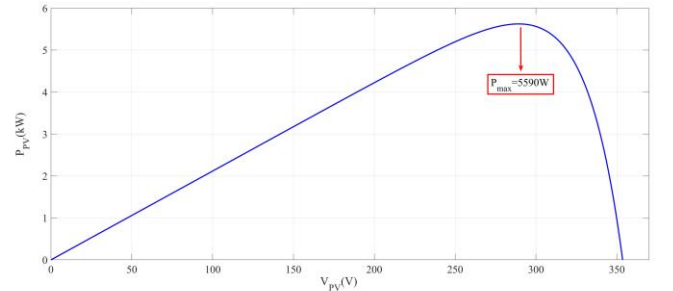


Fig. 7. Power-Voltage characteristic curves of a PV module

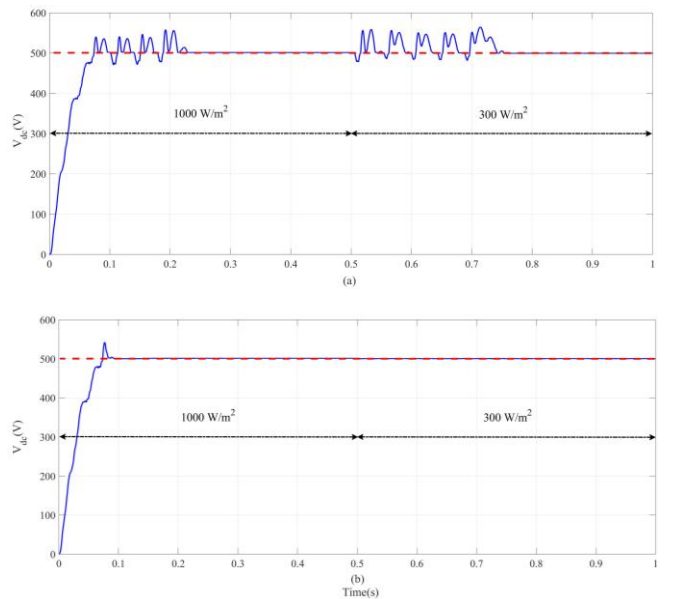


Fig. 8. dc link voltage with: a) PI controllers; b) Proposed controllers

Transient response of the proposed controller (MRAC-PI) is improved comparing with PI controller. Furthermore, PV system with the proposed controller is a robust system against uncertainty in irradiation. The steady state error of the system is also improved.

Direct axis current (I_d) in the presence of PI controller and proposed MRAC-PI controller when the irradiance is changed from 1000 W/m^2 to 300 W/m^2 at 0.5 Second are shown in Fig. 9.

The performance of the proposed controller (MRAC-PI) is robust and better than the results of PI controller facing with irradiation changes.

Quadrature axis current (I_q) controlled by PI controller and proposed MRAC-PI controller are illustrated in Fig 10.

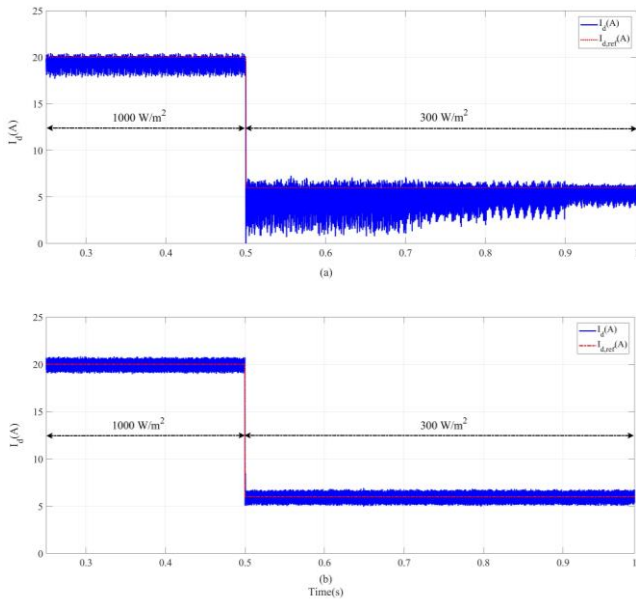


Fig. 9. d-axis grid current with: a) PI controllers; b) Proposed controllers

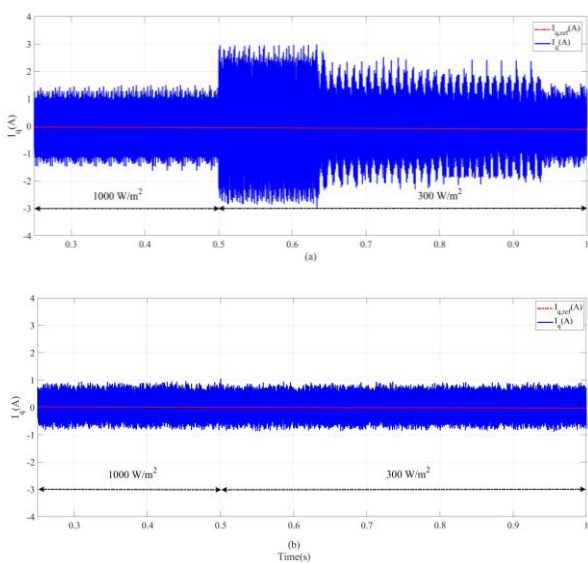


Fig. 10. q-axis grid current with: a) PI controllers; b) Proposed controllers

After change of irradiation in 0.5 Second, both controllers have a good steady state response. But between time of 0.5 to 0.8 Second, steady state response of PI controller has a larger tracking error.

Using grid current harmonic components analysis (THD), in the case of PI controller after change in irradiation, current THD of greater than 5% could be observed. In the case of proposed controller (MRAC-PI), THD is lower than 3% for whole simulation time. For irradiation of 1000 W/m^2 , THD is equal to 2.05% and in the case of irradiation of 300 W/m^2 , THD is 2.55%.

Output active power and injected active power to grid are shown in Fig. 11. This figure indicates that the boost converter controller, which is based on Beta algorithm, has a good performance in tracking maximum power point of the characteristic shown in Fig. 7. The equality of output active power of PV arrays (Fig. 11-a) and injected active power to the grid (Fig. 11-b), represents proper performance of boost converter and inverter controllers.

Phase voltage and phase current at connection point is shown in Fig. 12. Unit power factor at the connection point in large changes in irradiation confirms the robust performance of proposed controller.

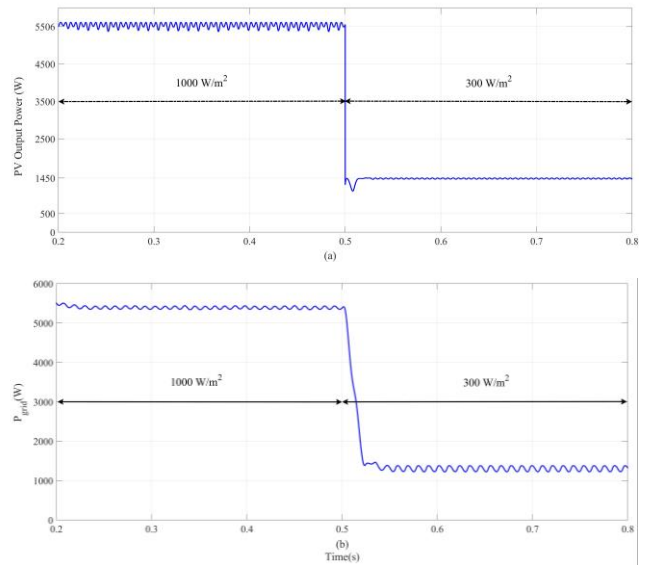


Fig.11. a) Extracting active power from PV arrays; b) Injection active power to grid

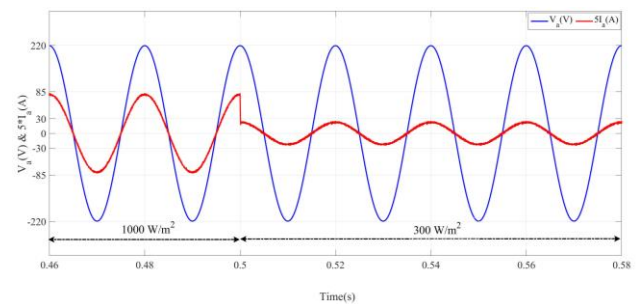


Fig.12. Grid voltage and grid current

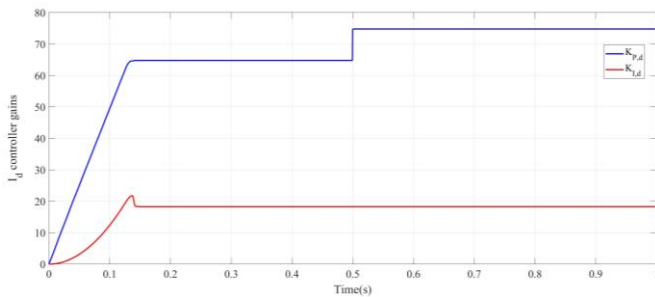


Fig. 13. d-axis current component, Proposed Controller coefficient

Fig. 13 shows the updated coefficients of the proposed controller (MRAC-PI) for controlling parameters of I_d . Coefficients of the MRAC-PI controller are updated in such a way that the considered reference values for controlling parameters of I_d , I_q , and V_{dc} are achieved due to reference model of (13).

The proposed control parameters change while facing with uncertainty occurrence, leads to robust operation of the control system.

V. CONCLUSION

In this paper a novel approach in utilizing MRAC-PI controlling algorithm (Fig. 6) is proposed for controlling on-grid PV system (Fig. 4). In this system three parameters of d and q components of grid current and dc link voltage are controlled to achieving a robust performance. Beta algorithm of Fig. 5 is applied for achieving maximizing power point tracking (MPPT) of PV arrays. It should be mentioned that this proposed controlling strategy has not been used for this purpose up to now. Proposed MRAC-PI controller with simple structure and based on MIT rule, estimates PI controller coefficients online. In order to analyze the performance of MRAC-PI controller, a change in irradiation is simulated and the results are compared with optimized PI controller by PSO algorithm. The proposed controller has a proper performance in the case of large signal variations. It should be noted in PI controllers the steady state error depends on open-loop gain. According to simulation results, proposed controller (Fig. 7) fulfills THD consideration of IEEE-519, adjusts grid power factor to unit accurately, decreases the transient response time, has robust performance in change of irradiance. Totally, it can be said that proposed algorithm has a better performance than optimized PI controller. The Beta method is can efficiently track the maximum power point in PV arrays.

REFERENCES

- [1] Renewable Energy Policy Network for the 21st Century (Ren21), *Renewables 2018 Global Status Report*, 2017.
- [2] U.S. department of energy, *2017 Renewable Energy Data Book*, 2017.
- [3] A. Anzalchi and A. Sarwat, "Overview of technical specifications for grid-connected photovoltaic systems," *Energy Conversion Magazine*, vol. 152, pp. 312-327, November 2017.
- [4] S. Kouro, J. I. Leon, D. Vinnikov and L. G. Franquelo, "Grid-Connected Photovoltaic Systems: An Overview of Recent Research and Emerging PV Converter Technology," in *IEEE Industrial on Electronics Magazine*, vol. 9, no. 1, pp. 47-61, March 2015.
- [5] G. Tsengenes and G. Adamidis, "A multi-function grid connected PV system with three level NPC inverter and voltage oriented control,"

Solar Energy Magazine, vol. 85, no. 11, pp. 2595-2610, November 2011.

- [6] Althobaiti, M. Armstrong, M. A. Elgendy and F. Mulolani, "Three-phase grid connected PV inverters using the proportional resonance controller," *2016 IEEE 16th International Conference on Environment and Electrical Engineering (EEEIC)*, Florence, pp. 1-6, June 2016.
- [7] J. Yang, S. Li, and X. Yu, "Sliding-Mode Control for Systems with Mismatched Uncertainties via a Disturbance Observer," *IEEE Trans. on Industrial Electronics*, vol. 60, no. 1, pp. 160-169, January 2013.
- [8] J. Hu, L. Shang, Y. He, and Z. Q. Zhu, "Direct Active and Reactive Power Regulation of Grid-Connected DC/AC Converters Using Sliding Mode Control Approach," *IEEE Trans. on Power Electronics*, vol. 26, no. 1, pp. 210-222, January 2011.
- [9] W. M. Naouar, A. Hemdani, E. Monmasson, I. Slama Belkhdja, L. Idkhajine, and M. Dagbagi, "Indirect sliding mode power control for three phase grid connected power converter," *IET Power Electronics*, vol. 8, no. 6, pp. 977-985, January 2015.
- [10] M. A. Mahmud, M. J. Hossain, H. R. Pota, and N. K. Roy, "Robust Nonlinear Controller Design for Three-Phase Grid-Connected Photovoltaic Systems Under Structured Uncertainties," *IEEE Trans. on Power Delivery*, vol. 29, no. 3, pp. 1221-1230, June 2014.
- [11] J. R. Massing, M. Stefanello, H. A. Gründling, and H. Pinheiro, "Adaptive Current Control for Grid-Connected Converters with LCL Filter," *IEEE Trans. on Industrial Electronics*, vol. 59, no. 12, pp. 4681-4693, December 2012.
- [12] R. V. Tambara, J. M. Kaniecki, J. R. Massing, M. Stefanello, and H. A. Gründling, "A Discrete-Time Robust Adaptive Controller Applied to Grid-Connected Converters with LCL Filter," *J. Control Automation Electronic System*, vol. 28, no. 3, pp. 371-379, January 2017.
- [13] S. Eren, M. Pahlevani, A. Bakhshai, and P. Jain, "An Adaptive Droop DC-Bus Voltage Controller for a Grid-Connected Voltage Source Inverter with LCL Filter," *IEEE Trans. on Power Electronics*, vol. 30, no. 2, pp. 547-560, February 2015.
- [14] R. M. Milasi, A. F. Lynch, and Y. W. Li, "Adaptive Control of a Voltage Source Converter for Power Factor Correction," *IEEE Trans. on Power Electronics*, vol. 28, no. 10, pp. 4767-4779, October 2013.
- [15] S. Oncu and S. Nacar, "Soft switching maximum power point tracker with resonant switch in PV system," *Int. J. Hydrog. Energy*, vol. 41, no. 29, pp. 12477-12484, August 2016.
- [16] S. Mohanty, B. Subudhi and P. K. Ray, "A Grey Wolf-Assisted Perturb & Observe MPPT Algorithm for a PV System," in *IEEE Transactions on Energy Conversion*, vol. 32, no. 1, pp. 340-347, March 2017.
- [17] M. A. G. de Brito, L. Galotto, L. P. Sampaio, G. d. A. e Melo and C. A. Canesin, "Evaluation of the Main MPPT Techniques for Photovoltaic Applications," in *IEEE Transactions on Industrial Electronics*, vol. 60, no. 3, pp. 1156-1167, March 2013.
- [18] S. Jain and V. Agarwal, "A new algorithm for rapid tracking of approximate maximum power point in photovoltaic systems," in *IEEE Power Electronics Letters*, vol. 2, no. 1, pp. 16-19, March 2004.